

Nonsmooth frequency shaping control design with an application

Alberto M. Simões* Pierre Apkarian** Dominikus Noll***

* ONERA-CERT, Control System Department, Toulouse, France (Tel: +33 5.62.25.27.64, email: alberto.simoies@cert.fr).

** ONERA-CERT, Control System Department, and Université Paul Sabatier, Institut de Mathématiques, Toulouse, France (Tel: +33 5.62.25.27.84, email: apkarian@cert.fr).

*** Université Paul Sabatier, Institut de Mathématiques, Toulouse, France (Tel: +33 5.61.55.86.22, email: noll@mip.ups-tlse.fr).

Abstract: Performance criteria of great practical interest in classical controller design are often expressed as constraints on specific frequency bands. This leads to a difficult design problem due to its inherent nonsmoothness and nonconvexity. In this paper, we present a rigorous approach based on constrained mathematical programming. The efficiency of our design technique is demonstrated with the practically difficult control of an uncertain flexible structure.

Keywords: structured controller design, nonsmooth optimization, flexible systems.

1. INTRODUCTION

Frequency shaping control design, also referred as multi-band design, consists in the simultaneous minimization of a finite family of closed-loop performance functions

$$f(K) = \max_{i=1, \dots, N} \|T_{w^i \rightarrow z^i}(K)\|_{I_i}, \quad (1)$$

where K is the feedback controller, $s \mapsto T_{w^i \rightarrow z^i}(K, s)$ stands for the i th closed-loop performance channel, and $\|T_{w^i \rightarrow z^i}(K)\|_{I_i}$ denotes the peak value of the transfer function maximum singular value norm on a prescribed frequency interval I_i :

$$\|T_{w^i \rightarrow z^i}(K)\|_{I_i} = \sup_{\omega \in I_i} \bar{\sigma}(T_{w^i \rightarrow z^i}(K, j\omega)).$$

The frequency band I_i is typically a closed interval $I_i = [\omega_1^i, \omega_2^i]$, or more generally, a finite union of intervals:

$$I_i = [\omega_1^i, \omega_2^i] \cup \dots \cup [\omega_{q_i}^i, \omega_{q_i+1}^i],$$

where right interval tips may take infinite values. Minimizing $f(K)$ for a single channel, $N = 1$ and $I_1 = [0, \infty]$, reduces to standard H_∞ synthesis.

Multi-band design is of great practical interest since performance criteria are often expressed as constraints on specific frequency bands. Currently these bands are handled indirectly by introducing weighting functions. This is inconvenient since finding the appropriate functions is time-consuming and prone to failure. Also, those functions increase the plant order and thereby the controller order, a potential source of numerical trouble and undesirable for hardware implementation. Our approach dispenses with weighting functions and thus avoids those difficulties.

* This research was supported by grants from Agence Nationale de Recherche (ANR) under contract *Guidage*, by Fondation d'entreprise EADS under contract *Solving challenging problems in feedback control*, and by ANR under contract *Controvert*.

Despite its importance, only few methods for multi-band synthesis are reported in the literature. In Iwasaki and Hara [2005], an extension of the Kalman-Yakubovich-Popov Lemma is developed for band restricted frequency domain constraints, but a fairly conservative convexifying procedure is adopted so that standard semidefinite programming solvers can be used. The QFT method [Horowitz, 1982] may be used to solve band limited synthesis problems, but it is no longer suited if additional structural constraints on the controller have to be satisfied. Similar comments could be made about synthesis methods based on the Youla parametrization, which generally lead to high-order controllers [Boyd et al., 1990]. Other tools, as the classical Bode, Nyquist and Nichols plots, and more recently in Toivonen and Totterman [2006], unfortunately are mainly limited to single-input single-output systems.

Our multi-band algorithm expands on the nonsmooth H_∞ synthesis method of Apkarian and Noll [2006]. As a substantial part of the computations is carried out in the frequency domain, where the plant state dimension only mildly affects algorithmic complexity, it allows highly efficient function and gradient calculations. Also, nonsmooth optimization avoids the presence of Lyapunov variables that leads to large size optimization programs as soon as systems get sizable and is one of the principal difficulties of linear or bilinear matrix inequalities.

The algorithm proposed here models closed-loop stability as a programming constraint, whenever the frequency bands used for performance do not fully cover the frequency axis, as will be clarified later. That means that it does not require the management of penalty or homotopy parameters as was still necessary in Apkarian and Noll [2007], and represents a more rigorous approach.

The efficiency of our design technique is demonstrated in a practically difficult case study involving the control of

a flexible telescope system. Frequency-domain constraints arise naturally in such systems due to the presence of flexible modes. While in traditional approaches the plant and weighting functions are assembled into a unique synthesis interconnection, our approach allows to keep each frequency band constraint explicitly, and to address the problem in a direct and natural way.

NOTATION

Let $\mathbb{R}^{n \times m}$ be the space of $n \times m$ matrices, equipped with the corresponding scalar product $\langle X, Y \rangle = X \bullet Y := \text{Tr}(X^T Y)$, where X^T is the transpose of the matrix X , $\text{Tr} X$ its trace. For complex matrices, X^H denotes the conjugate transpose. For Hermitian or symmetric matrices, $X \succ Y$ means that $X - Y$ is positive definite, $X \succeq Y$ that $X - Y$ is positive semi-definite. The symbol \mathbb{H}^m stands for the set of Hermitian matrices of size m . We let λ_1 denote the maximum eigenvalue of a symmetric or Hermitian matrix. The notation $\|\cdot\|$ will refer to the singular value matrix norm $\bar{\sigma}$, unless stated otherwise. The convex hull operation is denoted by $\text{co}\{\cdot\}$. For a locally Lipschitz function $f : \mathbb{R}^n \rightarrow \mathbb{R}$, $\partial f(x)$ denotes its Clarke subdifferential or generalized gradient at x , $f'(x; d)$ the Clarke directional derivative [Clarke, 1983]. For functions of two variables $f : \mathbb{R}^n \times \mathbb{R}^m \rightarrow \mathbb{R}$, the notation $\partial_1 f(x, y)$ is used to denote its Clarke subdifferential with respect to x at (x, y) . In the sequel, each $T_{w^i \rightarrow z^i}$ is a smooth operator defined on the open domain $\mathcal{D} \subset \mathbb{R}^{(m_2+k) \times (p_2+k)}$ of k th order stabilizing feedback controllers

$$K := \begin{bmatrix} A_K & B_K \\ C_K & D_K \end{bmatrix}, \quad A_K \in \mathbb{R}^{k \times k}$$

with values in the infinite dimensional space RH_∞ of rational stable transfer function matrices.

2. MULTI-BAND FREQUENCY DOMAIN DESIGN

We consider a plant P in state-space form

$$P(s) : \begin{bmatrix} \dot{x} \\ y \end{bmatrix} = \begin{bmatrix} A & B \\ C & D \end{bmatrix} \begin{bmatrix} x \\ u \end{bmatrix}$$

together with N concurring performance specifications, represented as a family of plants $P^i(s)$ described as

$$P^i(s) : \begin{bmatrix} \dot{x}^i \\ z^i \\ y^i \end{bmatrix} = \begin{bmatrix} A^i & B_1^i & B_2^i \\ C_1^i & D_{11}^i & D_{12}^i \\ C_2^i & D_{21}^i & D \end{bmatrix} \begin{bmatrix} x^i \\ w^i \\ u^i \end{bmatrix}, \quad i = 1, \dots, N, \quad (2)$$

where $x^i \in \mathbb{R}^{n^i}$ is the state vector of P^i , $u^i \in \mathbb{R}^{m_2}$ the vector of control inputs, $w^i \in \mathbb{R}^{m_1^i}$ the vector of exogenous inputs, $y^i \in \mathbb{R}^{p_2}$ the vector of measurements and $z^i \in \mathbb{R}^{p_1^i}$ the controlled or performance vector associated with the i th input w^i . The performance channels typically incorporate frequency filters which create new states x^i containing the state x of P , so that the matrices A^i contain the original system matrices A , etc. The difference with the usual multi-channel synthesis is that each $T_{w^i \rightarrow z^i}$ is only tested on a specific frequency band I_i . Without loss of generality, it is assumed throughout that $D = 0$.

The multi-band synthesis problem consists in designing a dynamic output feedback controller $u^i = K(s)y^i$ for the plant family (2) with the following properties:

- **Internal stability:** The controller K stabilizes the original plant P in closed-loop.
- **Performance:** Among all internally stabilizing controllers, K minimizes the worst case performance function $f(K) = \max_{i=1, \dots, N} \|T_{w^i \rightarrow z^i}(K)\|_{I_i}$.

The controller K has the frequency domain representation:

$$K(s) = C_K(sI - A_K)^{-1}B_K + D_K, \quad A_K \in \mathbb{R}^{k \times k}, \quad (3)$$

where k is the order of the controller, and where the case $k = 0$ of a static controller $K(s) = D_K$ is included. The synthesis problem may then be represented as

$$\begin{aligned} &\text{minimize } f(K) = \max_{i=1, \dots, N} \|T_{w^i \rightarrow z^i}(K)\|_{I_i} \\ &\text{subject to } K \text{ stabilizes } (A, B, C). \end{aligned} \quad (4)$$

Often practical considerations require additional structural constraints on the controller K . For instance, it may be desired to design low-order controllers ($0 \leq k \ll n_i$) or controllers with prescribed-pattern, PID control structures, and much else. Such structures are easily incorporated into program (4) as nonlinear programming constraints. Refer to Apkarian et al. [2007] for an example.

A difficulty in (4) is that stability is not a constraint in the usual sense of mathematical programming, because the set \mathcal{D} of closed loop stabilizing K is open, and an element K on the boundary $\partial \mathcal{D}$ is *not* a valid solution of the control problem. Since an optimization algorithm for (4) eventually converges to a solution on the boundary of \mathcal{D} , we have to modify this constraint in order to avoid numerical failure. Program (4) is therefore replaced by

$$\begin{aligned} &\text{minimize } f(K) = \max_{i=1, \dots, N} \|T_{w^i \rightarrow z^i}(K)\|_{I_i} \\ &\text{subject to } g(K) = \|(sI - \mathcal{A}(K))^{-1}\|_\infty - \beta^{-1} \leq 0 \end{aligned} \quad (5)$$

where $\mathcal{A}(K)$ is the closed-loop system matrix, and β is a small parameter. Notice that constraint $g(K) \leq 0$ will force the controller iterates to remain in the stabilizing region in the course of the algorithm. The value of $\beta > 0$ is the smallest distance to instability we allow the closed-loop system. In our experiments we usually choose $\beta \approx 10^{-9}$.

A normalization of practical interest for $f(K)$ in (5) is

$$f(K) = \max_{i=1, \dots, N} \|T_{w^i \rightarrow z^i}(K)\|_{I_i} / \gamma_i,$$

where the scalars γ_i are introduced to weigh the relative importance of the channels. In fact, if each γ_i is chosen as the maximum allowable value for the i th channel norm, then a final value $f(K) \leq 1$ indicates that an acceptable solution has been found.

3. NONSMOOTH MINIMIZATION TECHNIQUE

In this section we give a concise presentation of our optimization method. For a more detailed introduction to the salient features we refer the reader to Simões et al. [2008]. Our goal is to minimize a function of the form

$$f(K) = \max_{i=1, \dots, N} f_i(K),$$

where each $f_i(K)$ is a nonsmooth and nonconvex function of the form

$$f_i(K) = \sup_{\omega \in [\omega_{i1}, \omega_{i2}]} \lambda_1(T_{w^i \rightarrow z^i}(K, j\omega)T_{w^i \rightarrow z^i}(K, j\omega)^H).$$

Notice in this last expression that we have conveniently replaced f, f_i, g in (5) by their squares. In order to alleviate notation, we will henceforth write $f_i(K, \omega) = \lambda_1(T_{w^i \rightarrow z^i}(K, j\omega)T_{w^i \rightarrow z^i}(K, j\omega)^H)$, $T_i := T_{w^i \rightarrow z^i}$, and $S_i(K, \omega) = T_i(K, \omega)T_i(K, \omega)^H$.

Computing function values of each $f_i(K)$ can be based on the Hamiltonian algorithm of Boyd et al. [1989], which can be applied with minor changes to the case where the search for imaginary-axis Hamiltonian eigenvalues is restricted to the frequency band of interest. The Hamiltonian algorithm has to be applied to each $f_i(K), g(K)$ separately. It computes the function value, and the finite set of active frequencies or peaks in each window $[\omega_{i1}, \omega_{i2}]$.

The subgradients of $f_i(K)$ are of the form [Apkarian and Noll, 2006]

$$\Phi_Y^i = 2 \sum_{\omega \in \Omega_i(K)} \operatorname{Re}\{G_{21}^i(K, j\omega)T_i(K, j\omega)^H Q_\omega Y_\omega Q_\omega^H G_{12}^i(K, j\omega)\}^T, \quad (6)$$

where G_{12}^i and G_{21}^i are transfer functions computed through state-space realizations, and $\Omega_i(K) \subset [\omega_{i1}, \omega_{i2}]$ is the finite set of active frequencies of the i th channel T_i in the variable ω . Here Q_ω is a matrix whose columns form an orthonormal basis of the eigenspace of $T_i(K, j\omega)T_i(K, j\omega)^H$ associated with its maximum eigenvalue, and $Y_\omega \succeq 0$, $\sum_{\omega \in \Omega_i(K)} \operatorname{Tr}(Y_\omega) = 1$. The subgradient is for convenience indexed by $Y = (Y_\omega : \omega \in \Omega_i(K))$. In order to compute subgradients of f , we now have to take into account which of the indices $i = 1, \dots, N$ is active in the sense that $f_i(K) = f(K)$. Writing this set as $I(K)$, we obtain the subgradients $\Phi_{Y, \tau} \in \partial f(K)$ as

$$\Phi_{Y, \tau} = \sum_{i \in I(K)} \tau_i \Phi_Y^i, \quad \sum_{i \in I(K)} \tau_i = 1, \tau_i \geq 0, \quad \sum_{\omega \in \Omega_i(K)} \operatorname{Tr}(Y_\omega^i) = 1, Y_\omega^i \succeq 0. \quad (7)$$

Having explained in which way subgradients of the objective and constraint functions $f(K)$ and $g(K)$ are computed, let us now consider the program

$$\min\{f(K) : g(K) \leq 0\} \quad (8)$$

and investigate the generation of search steps. Following an idea in Polak [1997], we introduce the so-called progress function for (8):

$$F(K^+, K) = \max\{f(K^+) - f(K) - \mu g(K)_+; g(K^+) - g(K)_+\},$$

where $\mu > 0$ is some fixed parameter, and where $u_+ := \max\{u, 0\}$. We think of K as the current iterate, K^+ as the next iterate or as a candidate to become the next iterate. The following properties of the progress function are crucial for the understanding of our method. For a proof we refer to Apkarian et al. [2008].

Lemma 1. a) Suppose \bar{K} is a local minimum of program (8), then \bar{K} is also a local minimum of $F(\cdot, \bar{K})$. In particular, this implies $0 \in \partial_1 F(\bar{K}, \bar{K})$.

b) If \bar{K} satisfies the F. John necessary optimality conditions for (8), then $0 \in \partial_1 F(\bar{K}, \bar{K})$.

c) Conversely, if $0 \in \partial_1 F(\bar{K}, \bar{K})$, then \bar{K} is either a F. John critical point of (8), or it is a critical point of constraint violation.

We have used ∂_1 to denote the Clarke subdifferential with respect to the first variable. Notice here that \bar{K} is called a critical point of constraint violation of (8) if $g(\bar{K}) \geq 0$ and $0 \in \partial g(\bar{K})$. The interpretation of this is as follows. If $g(\bar{K}) > 0$, the constraint is violated. Moreover, $0 \in \partial g(\bar{K})$ says that \bar{K} is a local minimum (a critical point), so no progress toward the constraint can be made by moving from \bar{K} to some nearby point $\bar{K} + dK$. In other words, a point with these characteristics means failure to solve program (8). The case $g(\bar{K}) = 0, 0 \in \partial g(\bar{K})$ is of course the limiting case of the above. Here the point \bar{K} is feasible, but we cannot further optimize $f(K)$ in the neighborhood of \bar{K} , because the constraint will not let us move, as it becomes infeasible as soon as we try.

A consequence of Lemma 1 is that we should look for points \bar{K} satisfying $0 \in \partial_1 F(\bar{K}, \bar{K})$. For this we apply some sort of linearization procedure to the functions f and g . Writing $f_i(K)$ in the form

$$f_i(K^+) = \max_{\omega \in I_i} \lambda_1(S_i(K^+, \omega))$$

we introduce a first-order approximation of f in the neighbourhood of K :

$$\begin{aligned} \tilde{f}_i(K^+, K) &= \sup_{\omega \in I_i} \lambda_1(S_i(K, \omega) + S'_i(K, \omega)(K^+ - K)) \\ &= \sup_{\omega \in I_i} \sup_{Z_{\omega, i} \in \mathbb{B}_i} Z_{\omega, i} \bullet [S_i(K, \omega) + S'_i(K, \omega)(K^+ - K)], \end{aligned}$$

where $S'_i(K, \omega)$ is the Fréchet derivative of $S_i(\cdot, \omega)$ at K , $\mathbb{B}_i = \{Z \in \mathbb{H}^{m_i} : Z \succeq 0, \operatorname{Tr}(Z) = 1\}$, and where m_i is the size of $S_i = T_i T_i^H$. Associating \tilde{g} with g in a similar fashion, we obtain a first-order approximation for $F(K^+, K)$:

$$\tilde{F}(K^+, K) = \max \left\{ \max_{i=1, \dots, N} \tilde{f}_i(K^+, K) - f(K) - \mu g(K)_+; \tilde{g}(K^+, K) - g(K)_+ \right\}.$$

Notice that $\tilde{F}(K, K) = F(K, K)$, and that $\tilde{F}(K^+, K)$ is close to $F(K^+, K)$ for K^+ in a neighbourhood of K . Moreover, $\partial_1 \tilde{F}(K, K) = \partial_1 F(K, K)$, so we keep looking for points \bar{K} with $0 \in \partial_1 \tilde{F}(\bar{K}, \bar{K})$. It is convenient to write \tilde{F} somewhat differently. We put

$$\begin{aligned} \alpha_i(Z_{\omega, i}, \omega) &= Z_{\omega, i} \bullet S_i(K, \omega) - f(K) - \mu g(K)_+, \\ \Phi(Z_{\omega, i}, \omega) &= S'_i(K, \omega)^* Z_{\omega, i} \end{aligned}$$

for $i = 1, \dots, N$, and

$$\begin{aligned} \alpha_{N+1}(Z_{\omega, N+1}, \omega) &= Z_{\omega, N+1} \bullet S_{N+1}(K, \omega) - g(K)_+, \\ \Phi_{N+1}(Z_{\omega, N+1}, \omega) &= S'_{N+1}(K, \omega)^* Z_{\omega, N+1}. \end{aligned}$$

Then, putting $\mathcal{G} = \operatorname{co}\{(\alpha_i(Z_{\omega, i}, \omega), \Phi_i(Z_{\omega, i}, \omega)) : \omega \in I_i, Z_{\omega, i} \in \mathbb{B}_i, i = 1, \dots, N+1\}$, we have

$$\tilde{F}(K^+, K) = \max\{\alpha + \langle \Phi, K^+ - K \rangle : (\alpha, \Phi) \in \mathcal{G}\}.$$

Since \mathcal{G} is an infinite set, our last step is now to replace it by a finitely representable (and therefore computable) approximation $\hat{\mathcal{G}}$. This corresponds to replacing $\tilde{F}(K^+, K)$ by the approximation $\hat{F}(K^+, K)$ defined as

$$\hat{F}(K^+, K) = \max\{\alpha + \langle \Phi, K^+ - K \rangle : (\alpha, \Phi) \in \hat{\mathcal{G}}\}.$$

The role of $\hat{\mathcal{G}}$ is to render the tangent program numerically tractable. It consists in choosing a finite set of frequencies,

$\omega \in \Omega_e^i(K) \subset I_i$, and letting the $Z_{\omega,i} \in \mathbb{B}_i$ take a specific form.

We construct \widehat{G} as follows. Define $f_{N+1}(K) := g(K)$ and for every $i = 1, \dots, N + 1$ take the finite set $\Omega^i(K)$ of active frequencies of $f_i(K)$ at K . In other words, $f_i(K) = f_i(K, \omega)$ for $\omega \in \Omega^i(K)$. Now for every i add finitely many nearly active frequencies to those in $\Omega^i(K)$ to obtain an extended set of $\omega \in \Omega_e^i(K)$. Notice that $f_i(K, \omega) < f_i(K)$ for $\omega \in \Omega_e^i(K) \setminus \Omega^i(K)$. Now pick for each i and for every $\omega \in \Omega_e^i(K)$ an orthonormal basis $Q_{\omega,i}$ of the eigenspace of $f_i(K, \omega) = \lambda_1(S_i(K, \omega))$ at K , so that $\partial f_i(K, \omega) = \{S_i'(K, \omega)^* [Q_{\omega,i} Y_{\omega,i} Q_{\omega,i}^H] : Y_{\omega,i} \succeq 0, \text{Tr}(Y_{\omega,i}) = 1\}$. In other words, $Z_{\omega,i} = Q_{\omega,i} Y_{\omega,i} Q_{\omega,i}^H$ reduces the degrees of freedom from $m_i(m_i + 1)/2$ in the class of all $Z_{\omega,i}$ to the smaller size of $Y_{\omega,i}$. Include all these elements $\Phi = S_i'(K, \omega)^* [Q_{\omega,i} Y_{\omega,i} Q_{\omega,i}^H]$ with their corresponding terms $\alpha_i(Z_{\omega,i}, \omega)$ among \widehat{G} . As the matrix $Q_{\omega,i}$ is fixed, it is convenient to index them as $\Phi_i(Y_{\omega,i}, \omega)$ and $\alpha_i(Y_{\omega,i}, \omega)$, where $\omega \in \Omega_e^i(K)$ and $Y_{\omega,i} \succeq 0, \text{Tr}(Y_{\omega,i}) = 1$ has the appropriate size, and $i = 1, \dots, N + 1$. The index $i = N + 1$ adds the corresponding elements for the constraint g .

Having defined \widehat{G} and therefore $\widehat{F}(K^+, K)$, we solve the tangent program

$$\min_{dK} \widehat{F}(K + dK, K) + \frac{\delta}{2} \|dK\|^2. \quad (9)$$

Refer to Simões et al. [2008] for an detailed discussion on how (9) is solved. The solution being dK , we check whether $K^+ = K + dK$ is acceptable. If this is not the case, we perform a backtracking linesearch until $K^+ = K + tdK$ satisfies the Armijo condition

$$F(K + tdK, K) - F(K, K) < \gamma t F'(\cdot, K)(K; dK) < 0$$

for some fixed $0 < \gamma < 1$. The crucial facts about (9) have been established in Apkarian and Noll [2006], and we state them here without proof:

- As soon as the solution dK of (9) is nonzero, dK is a descent direction of $F(\cdot; K)$ at K . On the other hand, if the solution is $dK = 0$, then $0 \in \partial_1 F(K, K)$.
- The Armijo line search can be arranged to find a successful step after finitely many trials.

Finally, our nonsmooth algorithm can be summarized as:

Algorithm 1 Nonsmooth algorithm for program (8)

Parameters: $\delta > 0, 0 < \beta, \gamma < 1$.

- 1: **Initialize.** Choose closed-loop stabilizing K^1 .
- 2: **Stopping test.** If $0 \in \partial_1 \widehat{F}(K^j, K^j)$ then stop. Otherwise continue.
- 3: **Compute descent direction.** At counter j solve tangent program

$$\min_{dK} \widehat{F}(K^j + dK, K^j) + \frac{\delta}{2} \|dK\|^2.$$

Solution is the search direction dK .

- 4: **Line search.** Find $t = \beta^\nu, \nu \in \mathbb{N}$, satisfying the Armijo condition

$$F(K^j + tdK, K^j) - F(K^j, K^j) \leq \gamma t F'(\cdot, K^j)(K^j, dK).$$

- 5: **Update.** Put $K^{j+1} = K^j + tdK$, increase counter j by 1 and loop back to step 2.
-

Notice that this algorithm is in the class of so-called phase-I-phase-II methods. As long as the constraint $g(K) \leq 0$ is not satisfied, the second term in \widehat{F} is dominant and reducing \widehat{F} amounts to reducing constraint violation. This is phase I, which ends successfully once a feasible iterate $g(K^j) < 0$ has been found. This is where phase II begins. From now on iterates stay feasible, and the objective function is minimized at each step. In that case the algorithm converges toward a critical point of (8). Refer to Apkarian et al. [2008] for the proof. If $g(K^j) > 0$ for all j , then the algorithm converges to a critical point of constraint violation. In that case which occurs rarely in practice when constraints are feasible, a restart becomes necessary.

4. LINE-OF-SIGHT REGULATION OF A FLEXIBLE STRUCTURE

The case study we consider now involves the continuous control of the elevation axis of the telescope mock-up described in Alazard et al. [1996], consisting of a gimbal system mounted on flexural pivots. The primary objective is Line-of-Sight(LOS) regulation in an inertial reference coordinate system against motions of the supporting base.

The block diagram representation of the set-up is shown in Fig. 1, where θ_s and $\dot{\theta}_s$ are the inertial position and velocity of the supporting base, $\theta_p, \dot{\theta}_p$ and $\ddot{\theta}_p$ are the inertial position, velocity and acceleration of the telescope, u is the control torque, θ_p^m and $\ddot{\theta}_p^m$ are the measured inertial position and acceleration of the telescope, and $\ddot{\theta}_0$ represents the accelerometer bias. In the structural dynamic model, $g(s)$ is an identified transfer function of order 40, comprising the flexible modes of the telescope. The stiffness and friction feedbacks, k_b and f_b , model the flexible bearings. Magnitudes of the open-loop transfer functions $u \rightarrow \theta_p^m$ and $u \rightarrow \ddot{\theta}_p^m$ are shown in Fig. 2.

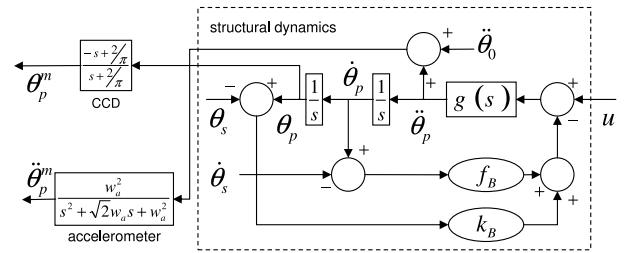


Fig. 1. block-diagram representation of the telescope

Design specifications for this application are very demanding. In order to assure high quality LOS stabilization, the controller must achieve good disturbance rejection over a wide frequency range. Secondly, the closed-loop system must be robust to uncertainties due to the identification phase and to variations of the mechanical impedance of the supporting base. Also, accelerometer bias should be rejected. Finally, a simple low-order controller is sought to facilitate on-board implementation.

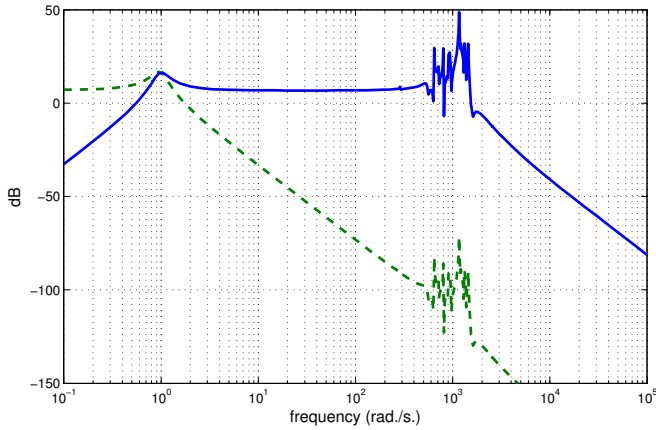


Fig. 2. open-loop $T_{u \rightarrow \ddot{\theta}_p^m}$ (solid) and $T_{u \rightarrow \theta_p^m}$ (dashed)

In traditional H_2 or H_∞ syntheses, performance and robustness specifications have to be gathered into a single criterion, which requires appending inputs and outputs of all channels. This introduces artificial crossed channels that do not reflect useful specifications. Since these cross channels are optimized along with the genuine interconnections, this approach increases conservatism. Also, traditional synthesis methods yield only full-order controllers, so that whenever simplicity is of prior importance, either a reduced plant model must be constructed or the controller has to be reduced afterwards. A further weakness of the classical approach is that weighting functions must be knitted to achieve flexible modes attenuation and reject the accelerometer bias.

With our proposed multi-band technique, each of the design specifications can be addressed individually. Since the controller order and structure can be specified explicitly and are independent of the system dimension, there is no need to reduce plant or controller. The performance and robustness specifications are simply expressed through band-restricted performance constraints:

- **LOS regulation:** decoupling with respect to motions of the supporting base can be achieved by forcing the magnitude of the disturbance transfer function $T_{\theta_s \rightarrow \theta_p} = \theta_p(s)/\theta_s(s)$ to be very small on the frequency range of interest:

$$|T_{\theta_s \rightarrow \theta_p}| \leq -70 \text{ dB, for } \omega \in I_1 := [0, 2e3] \text{ rad./s.}$$

- **Robustness:** robustness to unstructured uncertainties in the intermediate frequency range is achieved by frequency shaping of the sensitivity function $\tilde{S} = (I + KP)^{-1}$, where P is the plant in Figure 1. As is well known, the magnitude of the sensitivity function

$$|\tilde{S}| = |(I + KP)^{-1}| = \frac{1}{|1 + KP|}$$

represents the inverse of the distance to the critical point, so that minimizing $|\tilde{S}|$ turns out equivalent to maximizing the stability margin. The associated restricted-band constraint is given as

$$|\tilde{S}| \leq 1.5, \text{ for } \omega \in I_2 := [10, 400] \text{ rad./s.}$$

- **Attenuation of flexible modes:** by a similar reasoning, the magnitude of the sensitivity function is limited in the frequency range of the flexible modes:

$$|\tilde{S}| \leq 1.3, \text{ for } \omega \in I_3 := [400, 2e4] \text{ rad./s.}$$

However, this constraint alone is not enough to guarantee robustness with respect to variation of the flexible modes, because sensitivity reduction often induces pole-zero cancellation. This is clearly unacceptable since identified flexible modes are subject to uncertainties and also since the mechanical impedance of the supporting base may undergo large deviations. This is taken into account by prescribing a maximum roll-off in the frequency range of interest: a channel $w \rightarrow z^u$ is defined as:

$$P^u(s) : \begin{bmatrix} \dot{x} \\ z^u \\ \begin{bmatrix} \theta_p^m \\ \dot{\theta}_p^m \end{bmatrix} \end{bmatrix} = \begin{bmatrix} A & 0 & B_2 \\ 0 & 0 & 1 \\ C_2 & \begin{bmatrix} 0 \\ 1 \end{bmatrix} & D \end{bmatrix} \begin{bmatrix} x \\ w \\ u \end{bmatrix},$$

closed-loop the channel $w \rightarrow z^u$ will be equivalent to the transfer function $\dot{\theta}_p^m \rightarrow u$ of the controller. This is motivated by the fact that the flexible modes are relevant only through the accelerometer channel $u \rightarrow \ddot{\theta}_p^m$, as can be seen in Fig. 2. Thus, robustness with regard to flexible modes can be achieved by forcing the transfer function $\dot{\theta}_p^m \rightarrow u$ of the controller to be very small in the flexible modes frequency range: $|T_{w \rightarrow z^u}| \leq -50 \text{ dB, for } \omega \in I_4 := [5e2, 2e3] \text{ rad./s.}$

We note that the last specification above is equivalent to imposing a constraint directly on the controller gain, a thing which is not possible with more traditional Riccati or LMI H_∞ techniques. Such highly practical constraints are easy to handle with our nonsmooth optimization technique.

The first structural constraint imposed on the controller is its reduced order. A controller of order 14 is chosen. Secondly, the controller is forced to have a washout effect in the channel $\dot{\theta}_p^m \rightarrow u$ in order to reject the accelerometer bias. Finally, the controller is chosen strictly proper for better disturbances attenuation.

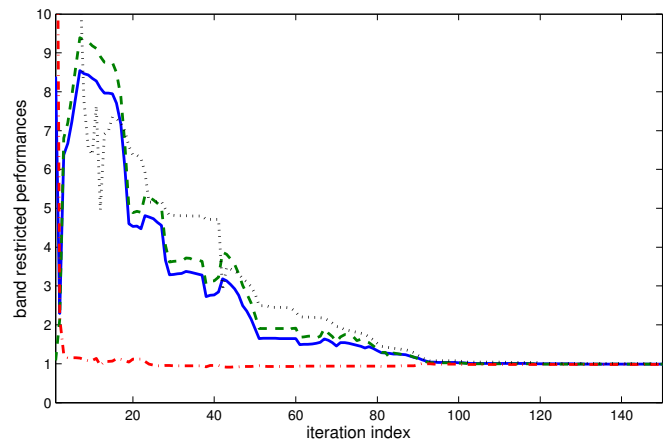


Fig. 3. evolution of band restricted performances vs. iteration index

Our telescope system in Fig. 1 has 45 states, structural and sensor dynamics included. Thus, the set comprising the 4 performance channels and the stability constraint correspond to a synthesis plant counting 225 states. The initial and final values of the normalized band-restricted norms $\bar{\gamma}_i$ for each performance channel are given in Table 1, while their evolution along the first 150 iterations is shown in Fig. 3. The algorithm takes 355 iterations in 26

minutes cpu to reach a local minimum within the allowed tolerance. However, a feasible solution meeting all design constraints is already available after 175 iterations.

We observe that the performance levels coalesce at the end of the iteration sequence, a strong indication that local optimality is reached. We also notice that the stability constraint $\|T_{stab}\|_\infty := \|(sI - \mathcal{A}(K))^{-1}\|_\infty \leq 10^9$ is not active and can probably be removed without much harm, which if done from scratch leads to significant speed-up. Numerical experience reveals that the stability constraint is only useful for problems involving few band constraints. It can usually be discarded when a sufficiently rich set of simultaneous specifications is considered.

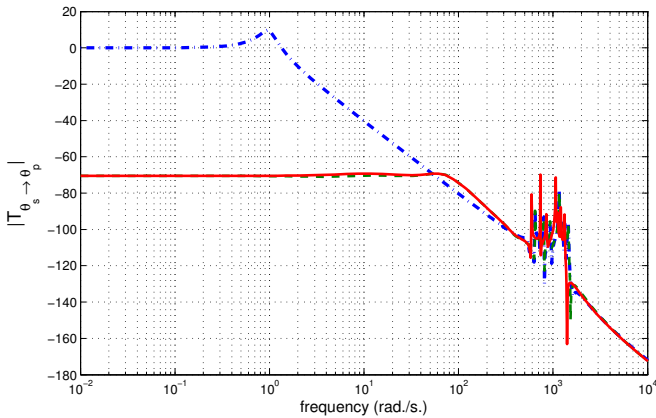


Fig. 4. magnitude of the transfer function $T_{\theta_s \rightarrow \theta_p}$ (solid: nominal closed-loop, dashed: perturbed closed-loop, dotted: nominal open-loop)

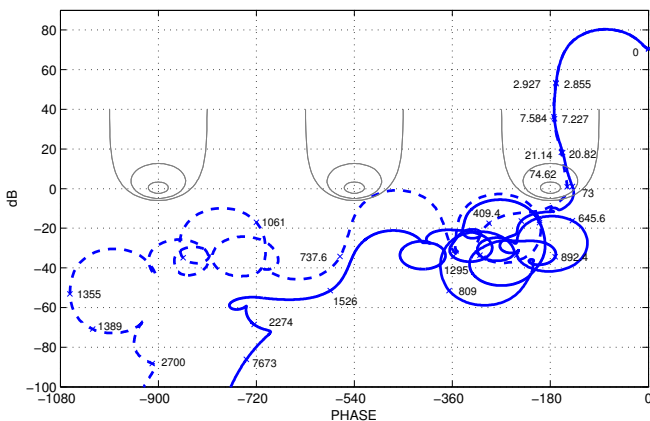


Fig. 5. Nichols diagram (solid: nominal system, dashed: perturbed system)

The closed-loop transfer function $T_{\theta_s \rightarrow \theta_p}$ is shown in Fig. 4. We observe an attenuation of 70 dB as specified. Fig. 5 shows the Nichols diagram for the closed-loop system. These figures also show the closed-loop responses of a 21-order perturbed model obtained by identification. The nominal and perturbed models differ significantly in the flexible modes range. However, since the magnitude of the transfer function $\theta_p^m \rightarrow u$ has been forced below -50 dB on the critical interval, and since the contribution of flexible modes through the channel $u \rightarrow \theta_p^m$ is negligible, the open-loop transfer function has magnitude always lower than unity, and the closed-loop system remains stable in both cases. See the Nichols plot in Fig. 5. All band restricted performances were achieved in the sense that $f(K) \leq 1$.

	$ T_{\theta_s \rightarrow \theta_p} $	$ \tilde{S} _{I_2}$	$ \tilde{S} _{I_3}$	$ T_{w \rightarrow z_u} $	$\ T_{stab}\ _\infty$
Initial	8.39	1.0863	24.533	51.65	548
Final	0.97966	0.98543	0.97776	0.98756	262

Table 1. final multi-band performances

5. CONCLUSION

We have discussed a nonsmooth algorithm for design problems subject to several band-restricted frequency domain constraints. Our approach is flexible in as much as it bypasses the difficult phase of selection of weighting function, and allows to handle a large variety of controller structures of practical interest. Application to the line-of-sight stabilization of a flexible telescope system demonstrates that the approach is an efficient practical design tool in challenging situations.

ACKNOWLEDGEMENTS

The authors would like to thank Professor Daniel Alazard (SUPAERO) for providing the telescope design problem.

REFERENCES

- D. Alazard, J.P. Chrétien, and M. Le Du. Attitude control of a telescope with flexible modes. In *Dynamic and Control of Large Structures in Space*, pages 15–19, London, UK, June 1996.
- P. Apkarian and D. Noll. Nonsmooth optimization for multiband frequency domain control design. *Automatica*, 43(4):724–731, April 2007.
- P. Apkarian and D. Noll. Nonsmooth H_∞ synthesis. *IEEE Trans. Aut. Control*, 51(1):71–86, 2006.
- P. Apkarian, V. Bompard, and D. Noll. Nonsmooth structured control design with application to PID loop-shaping of a process. *Int. J. Robust and Nonlinear Control*, 17(14):1320–1342, 2007.
- P. Apkarian, D. Noll, and A. Rondepierre. Mixed H_2/H_∞ control via nonsmooth optimization. *To appear in SIAM J. Control and Opt.*, 2008.
- S. Boyd, V. Balakrishnan, and P. Kabamba. A bisection method for computing the H_∞ norm of a transfer matrix and related problems. *Mathematics of Control, Signals, and Systems*, 2(3):207–219, 1989.
- S. Boyd, C. Barratt, and S. Norman. Linear controller design: Limits of performance via convex optimization. *Proc. IEEE*, 78(3):529–574, March 1990.
- F. H. Clarke. *Optimization and Nonsmooth Analysis*. Canadian Math. Soc. Series. John Wiley & Sons, New York, 1983.
- I. Horowitz. Quantitative feedback theory. *IEE Proc.*, 129-D(6):215–226, November 1982.
- T. Iwasaki and S. Hara. Generalized KYP lemma: Unified frequency domain inequalities with design applications. *IEEE Trans. Aut. Control*, 50(1):41–59, 2005.
- E. Polak. *Optimization : Algorithms and Consistent Approximations*. Applied Mathematical Sciences, 1997.
- A. M. Simões, P. Apkarian, and D. Noll. A nonsmooth progress function algorithm for frequency shaping control design. *To appear in IET Control Theory Appl.*, 2008.
- H. T. Toivonen and S. Totterman. Design of fixed-structure controllers with frequency-domain criteria: a multiobjective optimisation approach. *IEE Proceedings Control Theory and Applications*, 153(1):46–52, January 2006.